




REGULAR ARTICLE

Changes in the Electronic Structure of a Wurtzite Solid Solution Mn:ZnSeS  
Caused by Vacancies of Sulfur Atoms

S.V. Syrotyuk<sup>1,\*</sup> , M.K. Hussain<sup>2</sup>, R.A. Nakonechnyi<sup>1</sup>

<sup>1</sup> Lviv Polytechnic National University, 79013 Lviv, Ukraine

<sup>2</sup> Department of Electrical Power Techniques Engineering, AL-Hussain University College, 56001 Kerbala, Iraq

(Received 05 January 2025; revised manuscript received 20 February 2025; published online 27 February 2025)

The first stage of this work is the study of changes in the electronic structure of the ZnSeS solid solution due to the influence of the Mn impurity, which replaces the Zn atom. The second stage of the work is devoted to determining the changes in the electronic structure parameters of this material caused by the combined influence of the Mn impurity and the sulfur atom vacancy. The electronic structure of both materials was calculated within the DFT framework using the hybrid exchange-correlation functional PBE0. The structure of the solid solution was determined in two stages. In the first step, the unit cell parameters were optimized, and in the second one, the relaxation of the lattice parameters was performed, including repeated optimization of the internal coordinates of the atoms. All calculations were performed for the relaxed structural parameters. After the introduction of the Mn substitution impurity, the electronic energy spectra and densities of electronic states (DOS) were obtained. Significant changes in the electronic structure parameters due to the manganese impurity were revealed. It was found that the doped solid solution Mn:ZnSeS is a semiconductor for both electron spin polarizations. A significant decrease in the band gap was found, caused by a combined action of two point defects – a manganese impurity and a sulfur atom vacancy.

**Keywords:** ZnSeS solid solution, Mn impurity, Electronic energy bands, DOS, Magnetic moment, Anion vacancy.

DOI: [10.21272/jnep.17\(1\).01017](https://doi.org/10.21272/jnep.17(1).01017)

PACS numbers: 71.15.Mb, 71.20.Nr, 71.27. + a

1. INTRODUCTION

Zinc sulfide, a II-VI group compound semiconductor, is particularly suitable for use as host material for a large variety of dopants because of its wide band gap (3.75 eV).<sup>1</sup> It has been extensively studied for a variety of applications, e.g., in optical coatings, solid-state solar window layers, electrooptic modulators, photoconductors, field effect transistors, optical sensors, photocatalysts, electroluminescent materials, phosphors, and other light-emitting materials. In fact, ZnS has found special importance in thin-film electroluminescent devices, lasers, and flat-panel displays when doped with divalent manganese ions [1].

Photocatalysis, as a potential route to relieving environmental and energy issues, has been intensively applied for pollutant degradation, water splitting, and solar energy conversion. As a typical metal sulfide, ZnS, which has a large band gap, exhibits excellent photocatalytic capacity, owing to its strong oxidation and high negative potentials of excited electrons. However, the photocatalytic activity of ZnS is greatly affected by its structural and optical properties, especially defects such as sulfur vacancy, sulfur interstitial, zinc vacancy, and zinc interstitial. This may be ascribed to the crucial role of the lattice defects, exposed facets, and crystalline phases in dominating light harvesting capacity, regulating active sites or facets, and managing charge transfer kinetics.

Sulfur vacancies are introduced by allowing the orbital of the neighboring zinc atoms to relax. Sulfur vacancies not only induce the raising of the valence band position but also serve as photosensitization units and hole acceptors, enhancing the visible light response, charge carrier separation, and resistance to photo-corrosion. Hence, it is crucial to design and explore ZnS-based heterojunctions with efficient visible light sorption and affluent vacancy sites [2].

Zinc sulphide (ZnS) is a compound semiconductor with a wide direct band gap having *n*-type conductivity. It is considered a viable candidate for light-emitting diodes, electroluminescent devices, flat panel displays, infrared windows, sensors, lasers, and solar cells. Numerous methods, including electrochemical deposition, microemulsion, solvothermal, sol-gel, co-precipitation, combustion synthesis, pyrolysis, hydrothermal, laser ablation, and vapor deposition, have been used to fabricate ZnS nanostructures. The hydrothermal method is adaptable, productive, and able to be adjusted; it doesn't require milling or calcination, has low contamination, and is cost-effective. It also has a high ability to regulate the nucleation process [3].

Customizing the chromatic discharge of nanomaterials is crucial for their use in light-emitting screens, field emitters, lasers, sensors, and optoelectronic devices. ZnS nanocrystals exhibit blue, green, and orange emissions. The luminescence characteristics of ZnS particles have

\* Correspondence e-mail: [stepan.v.syrotyuk@lpnu.ua](mailto:stepan.v.syrotyuk@lpnu.ua)



been altered by doping with various transition elements and rare-earth metals. The optical characteristics are affected by defects, crystal structure, size, and shape. These studies show the ability to adjust several emission characteristics from pure ZnS nanocrystals with various defect features [3].

ZnS doped with various elements are creating a new era for both academic research and industrial applications. So, the optical properties of modified ZnS thin film will help us to find a suitable doping element for convenient deposition which may enhance the conductance and transmitting properties of the film. This review work has been carried out to explore the four-modification elements that constitute Cu, Ni, Co & Fe as descending order of atomic number corresponding to Zn, along with some potential applications considering the recent research work with other doping elements too such as Al, C, Pt etc. For example, FE, FET, Catalytic, Solar cell, Electroluminescence, Fuel cell, different sensors (Chemical sensors, Biosensors, Humidity sensors, light sensors, UV light sensors) and nanogenerators use ZnS thin film [4].

Peculiarities of the impact of transition 3d elements impurities on the electronic structure of wide-gap cubic crystals were studied in theoretical works [5-7].

ZnS and ZnSe crystals, doped with transition 3d elements, as promising materials for use in laser technology, are well-studied materials [8]. In this article we to investigate The structural and electronic properties of the solid solution alloy  $ZnSe_xS_{1-x}$  in the wurtzite structure have been studied employing density functional theory (DFT) in the generalized gradient approximation (GGA-PBE) [9].

However, there is very little information in scientific periodicals about the solid solutions ZnSeS with 3d transition impurities. The experimental work is devoted to the excitation wavelength tuning of luminescent  $Mn^{2+}$ -doped  $ZnS_xSe_{1-x}$  obtained by mechanically induced self-sustaining reaction [10].

However, there are very few publications dedicated to the electronic structure of solid solutions ZnTSeS, where T denotes the impurities of transitional elements. That is why the purpose of this study is to identify the changes in the electronic structure of wurtzite solid solutions T:ZnSeS caused by impurities of transition elements T. Only a few works have been published for these materials [11-13].

The problem of calculating the electronic structure of the wurtzite solid solution ZnSeS with an admixture of Mn and also with an S vacancy is relevant, and we proceed to its solution.

## 2. CALCULATION

### 2.1 The Structure Optimization

The electronic structure of ZnSeS solid solutions doped with Mn atoms was calculated using the ABINIT complex of programs [14] in two stages.

At the first stage, structural optimization was done, which also consisted of two steps. The first step was to optimize the lattice parameter, and the second was to find the precise coordinates of the atoms in the supercell. In order to save space, we present the optimization results for the  $Zn_4Se_1S_3$  supercell, which contains eight atoms. The corresponding results are shown in Table 1.

This work is devoted to a comparative study of two materials. The first one is a solid solution of ZnSeS with an admixture of Mn. In the second material, the vacancy of the sulfur atom is taken into account.

**Table 1** – An example of optimizing the structure of a smaller supercell of a  $Zn_4Se_1S_3$  solid solution

Coords	$x/a$	$y/b$	$z/c$
S initial	0	0	0.18737
S optimized	0	0	0.19273
S initial	0.33333	0.66667	0.43753
S optimized	0.33333	0.66667	0.43788
S initial	0	0	0.68737
S optimized	0	0	0.68232
Se initial	0.66667	0.33333	0.93753
Se optimized	0.66667	0.33333	0.93624
Zn initial	0	0	0
Zn optimized	0	0	0.00876
Zn initial	0.33333	0.66667	0.25003
Zn optimized	0.33333	0.66667	0.25268
Zn initial	0	0	0.50007
Zn optimized	0	0	0.49749
Zn initial	0.66667	0.33333	0.75003
Zn optimized	0.66667	0.33333	0.74183

As can be seen from Table 1, the optimized reduced  $z$ -coordinates ( $z/c$ ) the Zn atoms differ from the starting ideal values 0.0, 0.25, 0.5, 0.75, respectively. The optimized values of the lattice lengths have acquired the following values:  $a = b = 7.34112$ ,  $c = 24.07181$  a.u., respectively. The starting lattice lengths had the values  $a = b = 7.43513$ ,  $c = 24.42189$  a.u., respectively. For none of the atoms, the condition of fixing the reduced coordinates was not applied. And the lattice angles remained the same as in the ideal starting supercell, i.e.  $\alpha = \beta = 90$ ,  $\gamma = 120$  degrees, respectively. The Cartesian forces (0.000423, 0.000337, 0.000139, 0.00139, 0.000193, 0.0000965, 0.000486, 0.000691) eV/Å, acting on the three S, one Se and four Zn atoms, respectively, have been reached at the end of a final optimization loop. The pressure corresponding to the optimized structure is characterized by a value of 0.00001 GPa. The starting values of the Cartesian forces were equal to (0.0491, 0.0052, 0.1348, 0.0157, 0.7104, 0.0270, 0.0065, 0.6790) eV/Å, respectively. The corresponding starting pressure was characterized by the value of 1.0 GPa.

In this work, we performed calculations for the  $Zn_{31}Mn_1Se_8S_{24}$  and  $Zn_{31}Mn_1Se_8S_{23}$  supercells, containing 64 and 63 atoms, respectively.

### 2.2 Details of the Calculation Scheme

The calculation of the electronic structure for the supercells  $Zn_{31}Mn_1Se_8S_{24}$  and  $Zn_{31}Mn_1Se_8S_{23}$  have been done by means of the Abinit [14] code. Calculations of the electronic structure were performed here on the PAW basis (projector augmented waves) [15]. The PAW approach has common features with numerical methods and pseudopotentials.

The calculation scheme in the PAW approach consists of two steps. In the first step, the smooth pseudo-wave function  $|\tilde{\psi}_{\alpha\mathbf{k}}\rangle$  is calculated. The second step is devoted to finding the true all-electronic wave function  $|\psi_{\alpha\mathbf{k}}\rangle$  of the crystal necessary to obtain dipole matrix elements. It is the latter that allows calculating the kinetic coefficients and optical constants of materials. Here  $\alpha$  is a band index, and  $\mathbf{k}$  is a vector from the first Brillouin zone. The true all-electronic wave function is derived by acting of the operator  $\tau$  on the smooth pseudo-wave function [15],

$$|\psi_{\alpha\mathbf{k}}\rangle = \tau |\tilde{\psi}_{\alpha\mathbf{k}}\rangle. \quad (2)$$

This operator is built of functions obtained for the free atom. In particular, these functions are partial atomic waves  $\phi$ , pseudowaves  $\tilde{\phi}_i$  and projectors  $\tilde{p}_i$ . So, the operator  $\tau$  looks like this [15],

$$\tau = 1 + \sum_i (|\phi_i\rangle - |\tilde{\phi}_i\rangle) \langle \tilde{p}_i|. \quad (3)$$

The Schrödinger equation on the plane wave basis is represented by the Hamiltonian matrix  $H$ , from which the effective Hamiltonian  $H_{eff}$  is derived, namely

$$H_{eff} = \tau^\dagger H \tau. \quad (4)$$

The action of the  $H_{eff}$  operator on the pseudowave function gives the following equation:

$$H_{eff} |\tilde{\psi}_{\alpha\mathbf{k}}\rangle = \tau^\dagger \tau |\tilde{\psi}_{\alpha\mathbf{k}}\rangle = \varepsilon_{\alpha\mathbf{k}}, \quad (5)$$

showing the same energy spectrum  $\varepsilon_{\alpha\mathbf{k}}$ , derived from the Hamiltonian  $H$ :

$$H |\psi_{\alpha\mathbf{k}}\rangle = \varepsilon_{\alpha\mathbf{k}} |\psi_{\alpha\mathbf{k}}\rangle. \quad (6)$$

Here the effective Hamiltonian is derived from the all-electronic Hamiltonian  $H$ . The true all-electronic function  $\psi_{\alpha\mathbf{k}}$  is suitable for calculation the dipole matrix elements necessary to obtain the optical constants of crystals [16, 17] and the kinetic coefficients of semiconductors [18].

The strongly correlated 3d electrons of the Mn atom move in narrow energy bands and are characterized by large effective mass values. This means that the usual exchange-correlation functional PBE [19], which takes into account the gradient corrections of the electron density, is not suitable for an adequate description of 3d electrons. That is why we use the hybrid exchange-correlation functional PBE0 here. The latter is employed in the following form [20], namely

$$E_{xc}^{PBE0}[\rho] = E_{xc}^{PBE}[\rho] + \beta(E_x^{HF}[\Psi_{3d}] - E_x^{PBE}[\rho_{3d}]). \quad (5)$$

In this functional, the exchange-correlation energy of the 3d electrons of the Mn atom  $E_x^{PBE}$ , found in the GGA approximation, is partially removed, and the exchange

energy of the same electrons, found in the Hartree-Fock theory  $E_x^{HF}$ , is substituted in its place.

Namely, the PBE0 functional is a mixture of two exchange-correlation functionals. The first of them is the usual GGA functional. It is suitable for smoothly varying electron densities in space. The second term in Eq. (5) contains the Hartree-Fock energy, in which there is no self-interaction error, which is very large for electrons that move in narrow energy bands, namely 3d electrons. The mixing factor  $\beta$  is recommended to be 0.25 [19]. The importance of using the hybrid exchange-correlation functional PBE0 was confirmed in a recent study of a solid solution of ZnSeTe with an admixture of a chromium 3d element [20], including a cationic vacancy.

### 3. RESULTS AND DISCUSSION

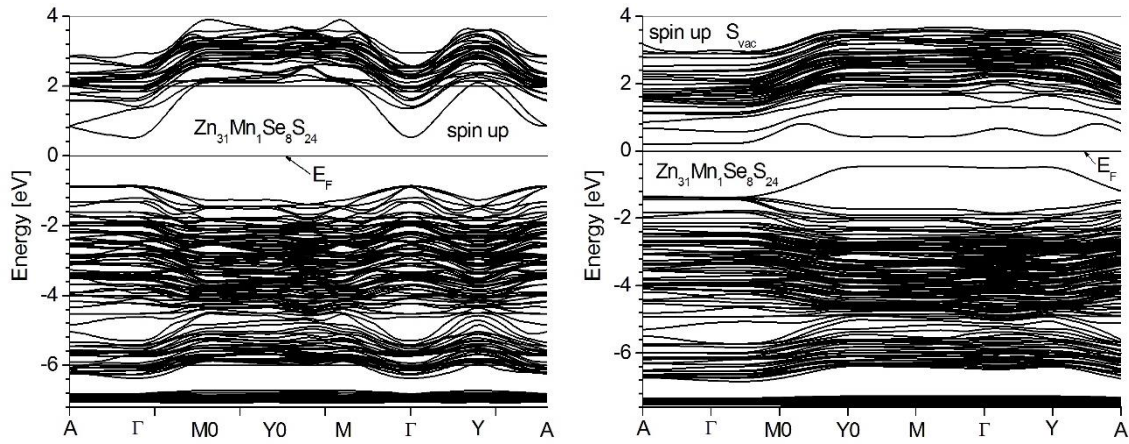
The calculated electronic properties of the Mn:ZnSeS solid solution in which the Mn atom replaces the Zn atom, are shown in Figures 1-5.

Fig. 1 shows the majority-spin electronic energy bands, evaluated for supercells  $\text{Zn}_{31}\text{Mn}_1\text{Se}_8\text{S}_{24}$ , without and with the S vacancy ( $V_S$ ). As can be seen from this Figure the Fermi level is situated within the forbidden band gap. So, the material Mn:ZnSeS represented by a supercell  $\text{Zn}_{31}\text{Mn}_1\text{Se}_8\text{S}_{24}$  reveals the semiconductor properties for the spin-up charge carriers. The band gap values for materials, without and with  $V_S$ , equal to 1.74 and 0.90 eV, respectively. Both materials are the direct-gap semiconductors. Fig. 2 shows the minority-spin electronic energy bands. As can be seen from Fig. 2 the Fermi level is also situated within the forbidden band gap. So, the materials Mn:ZnSeS represented by a supercell  $\text{Zn}_{31}\text{Mn}_1\text{Se}_8\text{S}_{24}$  reveal the semiconductor properties for the spin-down charge carriers, both without a vacancy and with a vacancy of a sulfur atom ( $V_S$ ). The band gap values for materials, without and with  $V_S$ , equal to 1.86 and 0.87 eV, respectively.

Curves in Fig. 3 reveal a significant asymmetry of the Mn d states, which indicates the presence of a non-zero magnetic moment of the supercell. For both supercells considered here, their total magnetic moments are  $5.0\mu_B$ , and the contributions of Mn atoms are also approximately equal and amount to  $3.8\mu_B$ .

The partial densities of states on Zn, Se and S atoms, presented in Fig. 4, show that the valence band is formed mainly by Se and S  $p$ -states. However, Zn atoms mainly delegate  $s$  states to the conduction zone. We also note in Fig. 3 narrow energy bands of d symmetry in the valence band, which are characterized by large values of the density of electronic states. For an adequate description of such states, we employ the PBE0 hybrid exchange-correlation functional. The usual GGA functional is unsuitable for describing electrons moving in narrow energy bands of d symmetry. It is these charge carriers that are characterized by a large amount of self-interaction energy, partially excluded in the PBE0 functional.

The asymmetry of the partial DOS curves, as well as the total density of electronic states (Fig. 5), is the result of the influence of the transition element Mn on the polarization of the electron density, even on such non-magnetic elements as Se and S.



**Fig. 1** – The majority-spin electronic energy bands, without and with a sulphur vacancy ( $S_{vac}$ ), evaluated for supercell  $Zn_{31}Mn_1Se_8S_{24}$

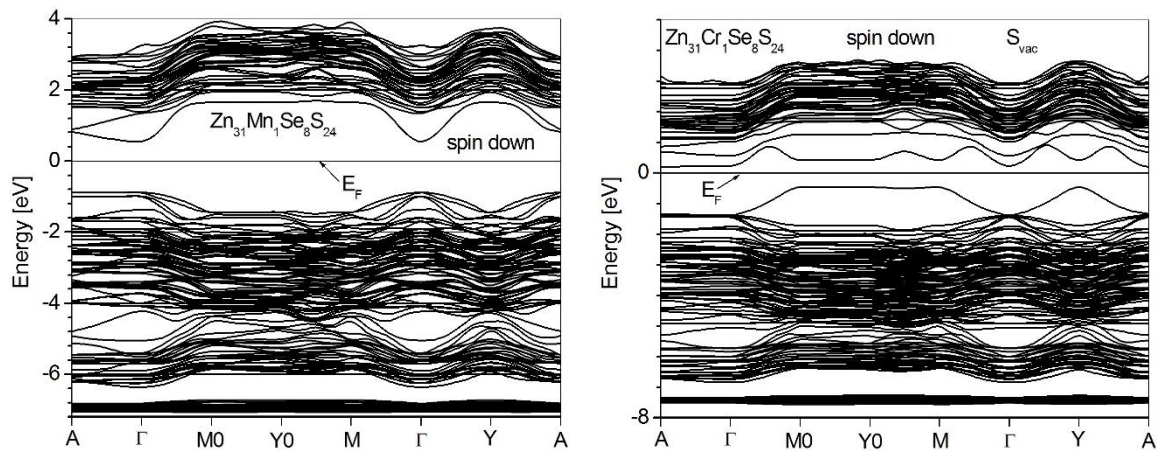


**Fig. 2** – The minority-spin electronic energy bands, without and with a sulphur vacancy ( $S_{vac}$ ), evaluated for supercell  $Zn_{31}Mn_1Se_8S_{24}$

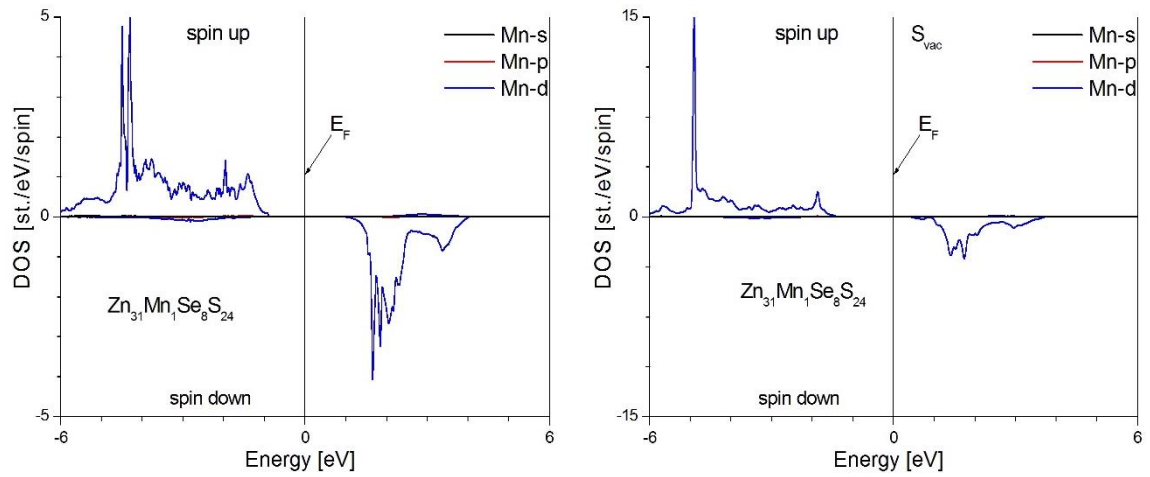


**Fig. 3** – The spin-resolved partial DOS, evaluated for supercell  $Zn_{31}Mn_1Se_8S_{24}$ , without and with a sulphur vacancy ( $S_{vac}$ )

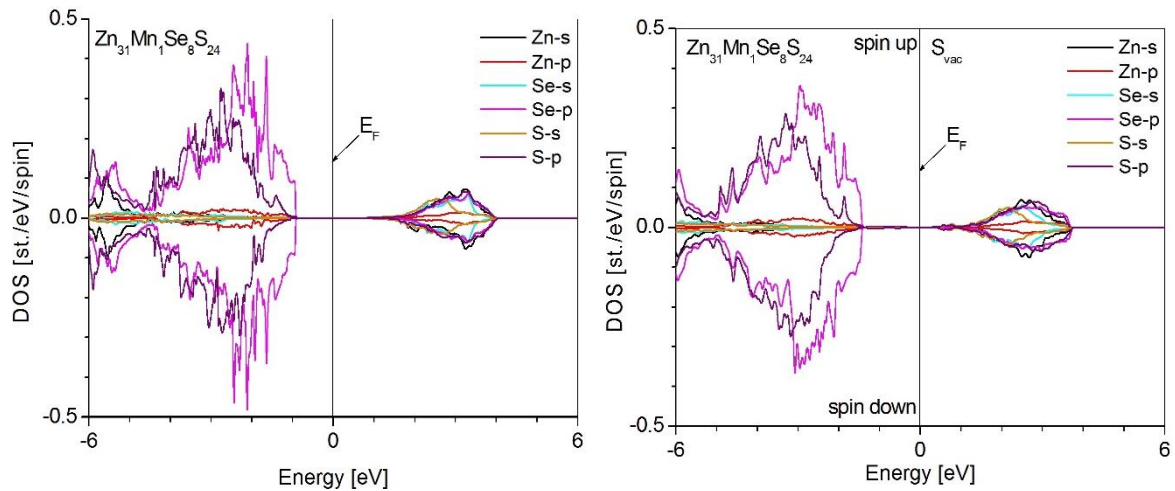


Fig. 4 – The spin-resolved partial DOS, evaluated for supercell  $Zn_{31}Mn_1Se_8S_{24}$ , without and with a sulphur vacancy ( $S_{vac}$ )

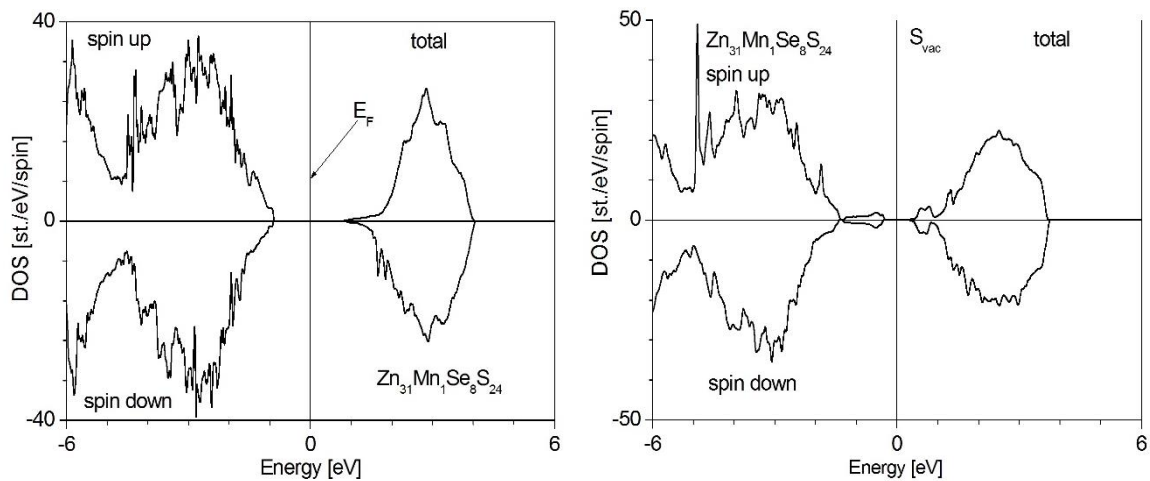


Fig. 5 – The spin-resolved total DOS, evaluated for supercell  $Zn_{31}Mn_1Se_8S_{24}$ , without and with a sulphur vacancy ( $S_{vac}$ )

#### 4. CONCLUSIONS

For the first time, the spin-polarized electronic structure of the Mn:ZnSeS solid solution is investigated. Electronic energy bands were evaluated for  $Zn_{31}Mn_1Se_8S_{24}$  and  $Zn_{31}Mn_1Se_8S_{23}$  supercells in which the Zn atom is replaced by the Mn atom. The second supercell represents a material with a Mn impurity and an S atom vacancy. The Mn impurity causes significant changes in the electronic structure of the ZnSeS solid solution. However, the introduction of an additional point defect, namely a vacancy at the S

atom site, leads to even greater changes in the electronic structure parameters. Thus, the band gap width for spin-up charge carriers decreases after the introduction of sulphur vacancies by 0.84 eV, and for spin-down states – by 0.99 eV, respectively.

#### ACKNOWLEDGEMENTS

This contribution was created under the support of the High Performance Computing Laboratory at the Lviv Polytechnic National University.

#### REFERENCES

1. S. Biswas, S. Kar, S. Chaudhuri, *J. Phys. Chem. B* **109**, 17526 (2005).
2. Hao Peng, Daixin Liu, Xiaogang Zheng, Xiaojin Fu, *Nanomaterials* **9**, 1657 (2019).
3. E.M. Jubeer, M.A. Manthrammel, P.A. Subha, M. Shkir, K.P. Biju, S.A. AlFaify, *Sci. Rep.* **13**, 16820 (2023).
4. A.M. Shakil, S. Das, A.M. Rahman, U.S. Akther, K.M. Hassan, K.M. Rahman, *Mater. Sci. Appl.* **9**, 751 (2018).
5. S.V. Syrotyuk, M.K. Hussain, *Phys. Chem. Solid State* **22**, 529 (2021).
6. S.V. Syrotyuk, O.P. Malyk, *J. Nano-Electron. Phys.* **11**, No 1, 01009 (2019).
7. S.V. Syrotyuk, O.P. Malyk, *J. Nano-Electron. Phys.* **11**, No 6, 06018 (2019).
8. S.B. Mirov, I.S. Moskalev, S. Vasilyev, V. Smolski, V.V. Fedorov, D. Martyshkin, J. Peppers, M. Mirov, A. Dergachev, V. Gapontsev, *IEEE J. Selected Topics Quantum Electron.* **24**, 1601829 (2018).
9. S. Sarkar, O. Eriksson, D. D. Sarma, I. Di Marco, *Phys. Rev. B* **105**, 184201 (2022).
10. M.A. Avilés, F.J. Gotor, *Opt. Mater.* **117**, 111121 (2021).
11. S.V. Syrotyuk, M.K. Hussain, *J. Nano-Electron. Phys.* **15**

- No 5, 05002 (2023).
12. S.V. Syrotyuk, A.Y. Nakonechnyi, Yu.V. Klysko, M.V. Stepanyak, V.M. Myshchysyn, *J. Nano- Electron. Phys.* **16** No 5, 05034 (2024).
  13. S.V. Syrotyuk, A.Y. Nakonechnyi, Yu.V. Klysko, Z.E. Veres, I.I. Lahun, *J. Nano- Electron. Phys.* **16** No 1, 01016 (2024).
  14. X. Gonze, F. Jollet, F. Abreu Araujo, D. Adams, B. Amadon, T. Applencourt, C. Audouze, J.-M. Beuken, J. Bieder, A. Bokhanchuk, E. Bousquet, F. Bruneval, D. Caliste, M. Cote, F. Dahm, F. Da Pieve, M. Delaveau, M. Di Gennaro, B. Dorado, C. Espejo, G. Geneste, L. Genovese, A. Gerossier, M. Giantomassi, Y. Gillet, D. R. Hamann, L. He, G. Jomard, J. Laflamme Janssen, S. Le Roux, A. Levitt, A. Lherbier, F. Liu, I. Lukacevic, A. Martin, C. Martins, M. J. T. Oliveira, S. Ponce, Y. Pouillon, T. Rangel, G.-M. Rignanese, A. H. Romero, B. Rousseau, O. Rubel, A. A. Shukri, M. Stankovski, M. Torrent, M. J. Van Setten, B. Van Troeye, M. J. Verstraete, D. Waroquier, J. Wiktor, B. Xu, A. Zhou, and J. W. Zwanziger, *Comput. Phys. Commun.* **205**, 106 (2016).
  15. P.E. Blöchl, *Phys. Rev. B* **50**, 17953 (1994).
  16. S.V. Syrotyuk, Yu.V. Klysko, *J. Nano- Electron. Phys.* **12** No 5, 05018 (2020).
  17. M. Boukhtouta, Y. Megdoud, S. Benlamari, H. Meradji, Z. Chouahda, R. Ahmed, S. Ghemid, Mohammed Abu-Jafar, S. Syrotyuk, D. P. Rai, S. Bin Omran, R. Khenata, *Philosoph. Magaz.* **100** No 9, 1150 (2020).
  18. O.P. Malyk, S.V. Syrotyuk, *J. Nano- Electron. Phys.* **14**, No 1, 01014 (2022).
  19. J.P. Perdew, K. Burke, M. Ernzerhof, *Phys. Rev. Lett.* **77**, 3865 (1996).
  20. F. Tran, P. Blaha, K. Schwarz, P. Novák, *Phys. Rev. B* **74**, 155108 (2006).

## Зміни електронної структури вюрцитного твердого розчину Mn:ZnSeS, зумовлені вакансіями атомів сірки

С.В. Сиротюк<sup>1</sup>, М.К. Hussain<sup>2</sup>, Р.А. Наконечний<sup>1</sup>

<sup>1</sup> Національний університет «Львівська політехніка», 79013 Львів, Україна

<sup>2</sup> Department of Electrical Power Techniques Engineering, AL-Hussain University College, 56001 Kerbala, Iraq

Першим етапом даного дослідження є вивчення змін електронної структури твердого розчину ZnSeS, зумовленої впливом домішки Mn, яка заміщує атом Zn. Другий етап роботи присвячений встановленню змін параметрів електронної структури цього матеріалу, спричинених сумісним впливом домішки Mn та вакансії атома сірки. Електронна структура обидвох матеріалів обчислювалась в рамках DFT з використанням гібридного обмінно-кореляційного функціоналу PBE0. Структура твердого розчину визначалась в два етапи. На першому кроці оптимізувались параметри елементарної комірки, а на другому виконувалась релаксація параметрів решітки, включаючи повторну оптимізацію внутрішніх координат атомів. Всі розрахунки були виконані для зреласованих структурних параметрів. Після введення домішки заміщення Mn були отримані електронні енергетичні спектри та густини електронних станів ГЕС (DOS). Виявлено суттєві зміни параметрів електронної структури, зумовлені домішкою марганцю. Було встановлено, що легований твердий розчин Mn:ZnSeS є напівпровідником для обидвох спінових поляризацій електронів. Виявлено значне зменшення ширини забороненої зони, знайдене за сумісної дії двох точкових дефектів – домішки марганцю і вакансії атома сірки.

**Ключові слова:** Твердий розчин ZnSeS, Домішка Mn, Електронні енергетичні зони, ГЕС (DOS), Аніонна вакансія.